On the Dynamic Stoichiometry of Metal Chalcogenide Nanocrystals: Spectroscopic Studies of Metal Carboxylate Binding and Displacement

Nicholas C. Anderson, Mark P. Hendricks, Joshua J. Choi and Jonathan S. Owen*

Department of Chemistry, Columbia University in the City of New York

New York, NY 10027.
Email: jso2115@columbia.edu

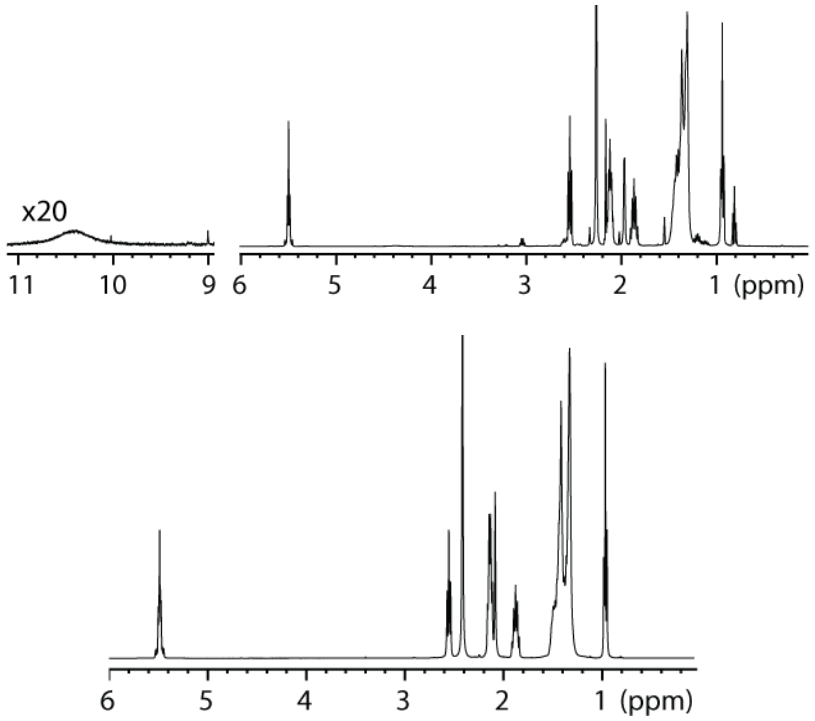

Figure S1: ^{1}H NMR spectrum of (κ^2-TMEDA)Cd(O_2CR)$_2$ isolated from CdSe nanocrystals after exposure to TMEDA (Top). Integration shows a 2:1 ratio of carboxylate and TMEDA in the isolated sample. Broad resonance at δ = 10.4 ppm is magnified 20x and corresponds to protonated TMEDA (coressponding to 8% of total carboxyls), formed by the reaction of TMEDA and carboxylic acid. The spectrum matches an independently prepared 1:1 mixture of cadmium oleate and TMEDA (bottom), with the exception of the acidic hydrogen visible at δ = 10.4 ppm.

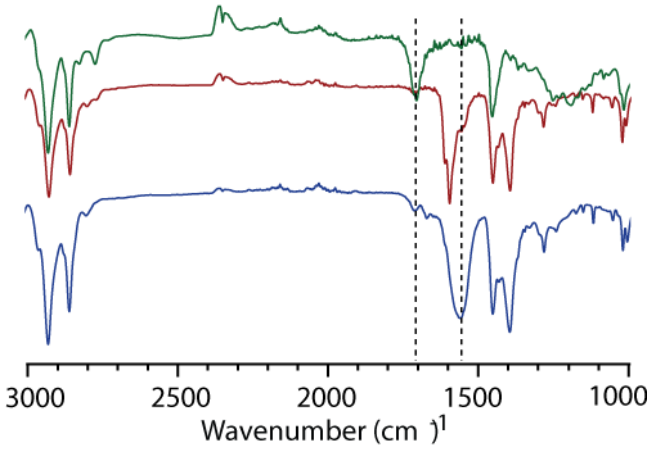

Figure S2. FT-IR spectra of (κ^2-TMEDA)Cd(O_2CR)$_2$ (R = oleyl, tetradecyl) isolated from CdSe nanocrystals after exposure to TMEDA (blue, bottom); an independently prepared mixture of oleic acid and TMEDA (green, top), and an independently prepared mixture of cadmium oleate and TMEDA (red, middle).

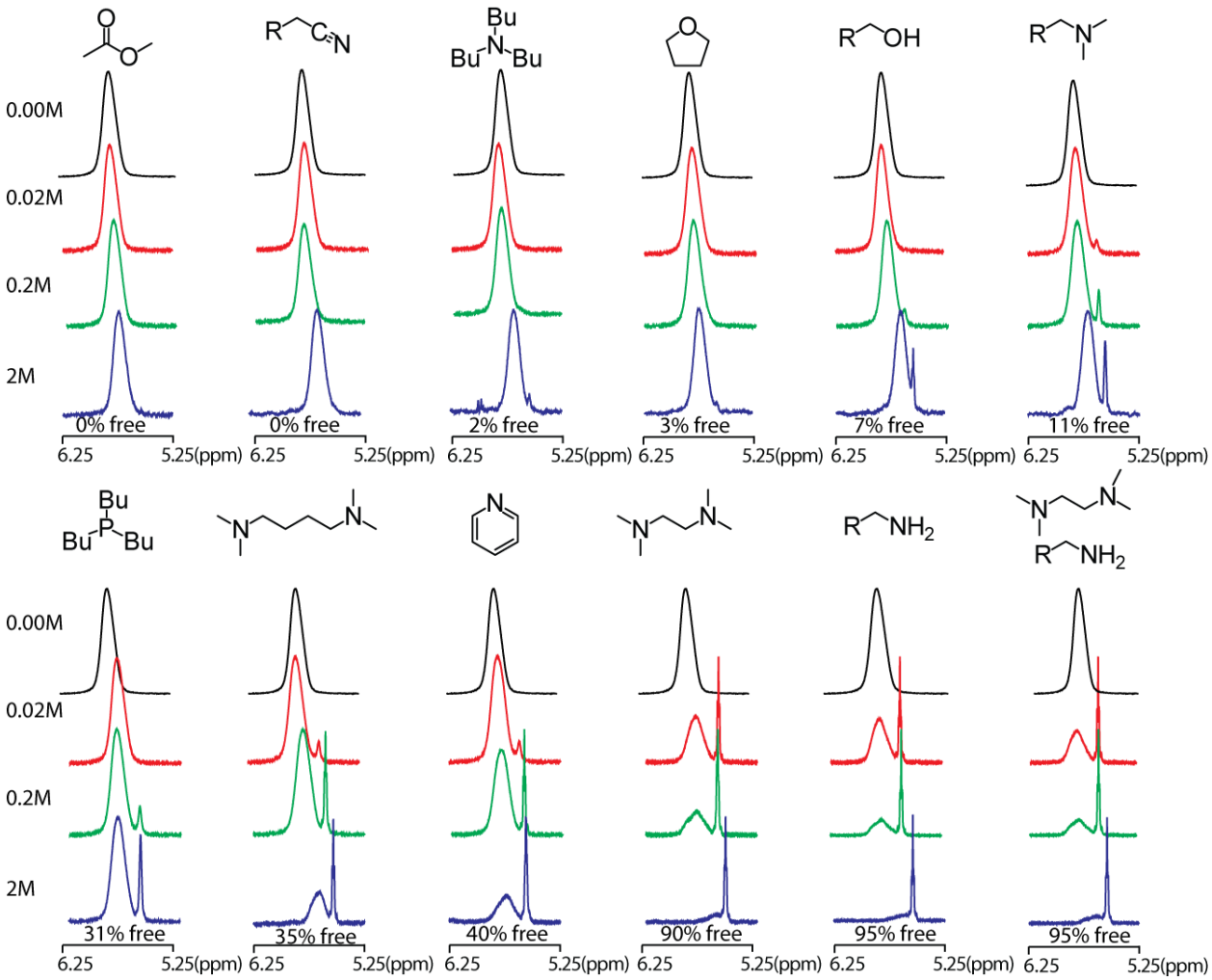

Figure S3: Vinyl region of the ^{1}H NMR spectra of CdSe nanocrystals (0.02 M in Carboxylate, see experimental section for more detail) with added Lewis bases (0.00 M (black, top), 0.02 M (red), 0.2 M (green), and 2.0 M (blue, bottom)). Appearance of sharp vinyl peak corresponds to displacement of L–Cd(O_2CR)$_2$. Percent free is calculated by integrating the sharp vinyl peak versus the full vinyl region. Numbers listed below each spectra correspond to the % displaced at 2.0 M. Changes to the chemical shifts of both free and bound signals at high concentration of ligand added may be due to a change in the dielectric of the solvent medium. The final 2M concentration is ~20% /volume added ligand. Similarly, as an increasing amount of Cd(O_2CR)$_2$ is removed from the nanocrystal the density of aliphatic ligands changes as does their local dielectric medium.

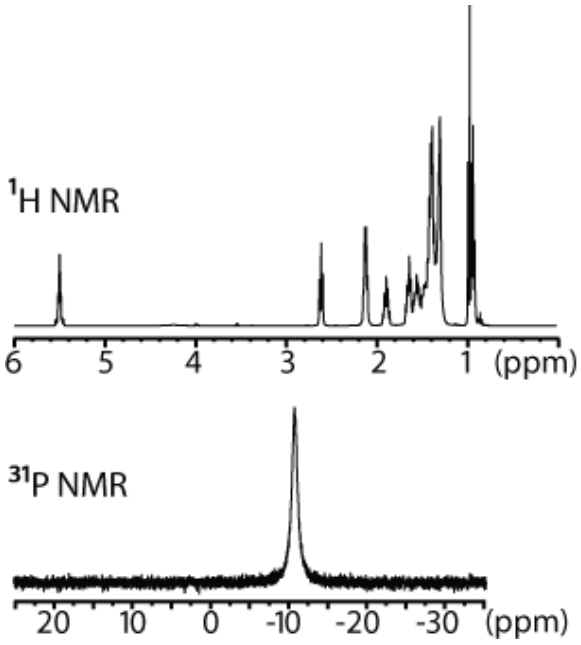

Figure S4. ^{1}H and ^{31}P NMR reference spectra of a 1:1 mixture of Bu_3P and cadmium oleate for comparison with Figure 2 in the main text. The ^{31}P chemical shift is downfield from the signal of free Bu_3P (= -12 vs. -31ppm). Furthermore, the resonance shifts further downfield as the concentration increses, perhaps due to the presence of rapidly inter-converting cadmium complexes with multiple phosphine ligands.

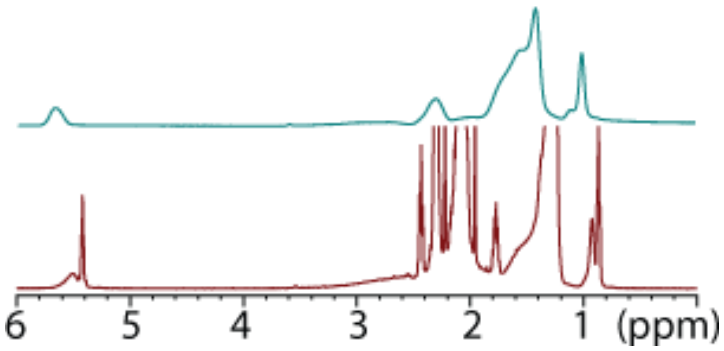

Figure S5. ^{1}H NMR spectrum of isolated carboxylate-terminated CdS nanocrystals (top, blue) treated with 2.0 M TMEDA in d_6-benzene (bottom, red). See experimental section for preparation of oleate-terminated CdS nanocrystals. Sharp peaks appear corresponding to the tetradecyl fragment of $(\kappa^2$-TMEDA)$Cd(O_2CR)_2$ displaced from the surface of the nanocrystal. Changes to the chemical shifts of both free and bound signals at high concentration of TMEDA added may be due to a change in the dielectric of the solvent medium. The final 2M concentration is ~20% /volume TMEDA. Similarly, as an increasing amount of $Cd(O_2CR)_2$ is removed from the nanocrystal the density of aliphatic ligands changes as does their local dielectric medium.

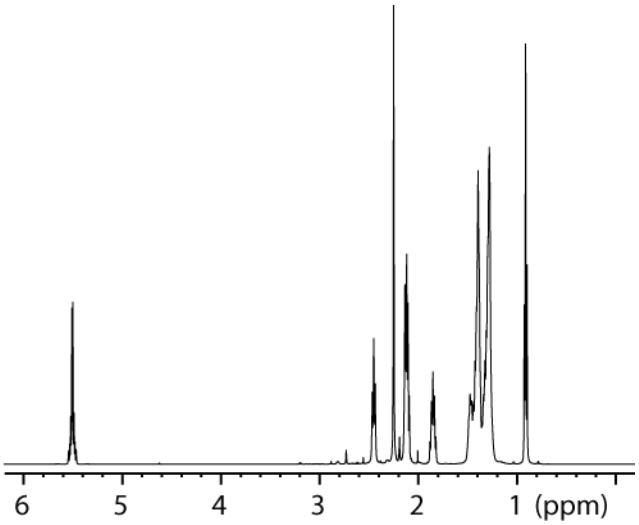

Figure S6A. ^{1}H NMR spectrum of (κ^2-TMEDA)Pb(O_2CR)$_2$ isolated from PbS nanocrystals. All peaks correspond to an independently prepared mixture of lead oleate and TMEDA. Integration of the resonances from the oleyl chain and TMEDA supports a 3:2 ratio of carboxylate to TMEDA.

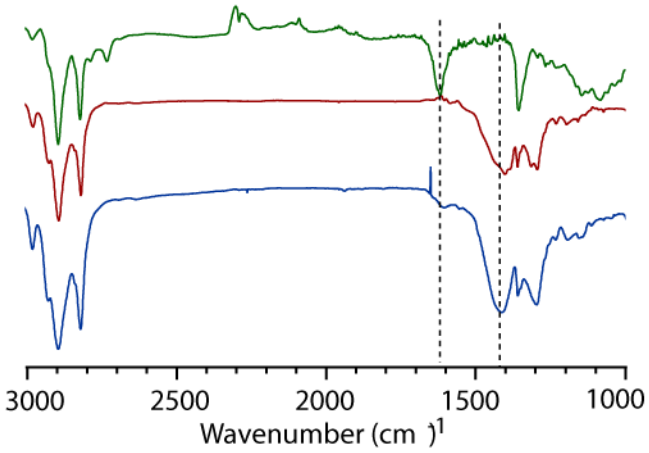

Figure S6B. FT-IR spectra of (κ^2-TMEDA)Pb(O_2CR)$_2$ (R = oleyl) isolated from PbS nanocrystals (blue, bottom), a mixture of oleic acid and TMEDA (green, top), and an independently prepared sample of (κ^2-TMEDA)Pb(O_2CR)$_2$ (red, middle).

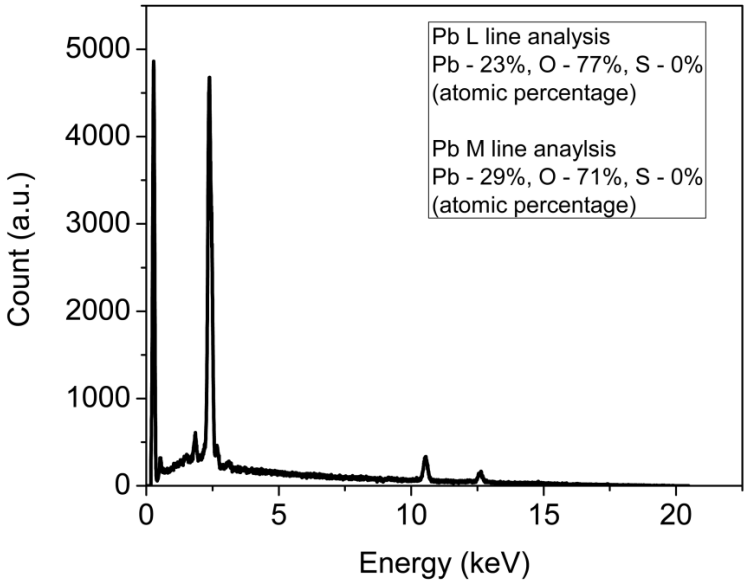

Figure S6C. Energy dispersive x-ray spectroscopy of (κ^2-TMEDA)Pb($O_2CR)_2$ (R = oleyl) isolated from PbS nanocrystals. The table shows the elemental composition calculated by peak fitting the EDX spectrum. The sample contains lead and oxygen but no sulfur.

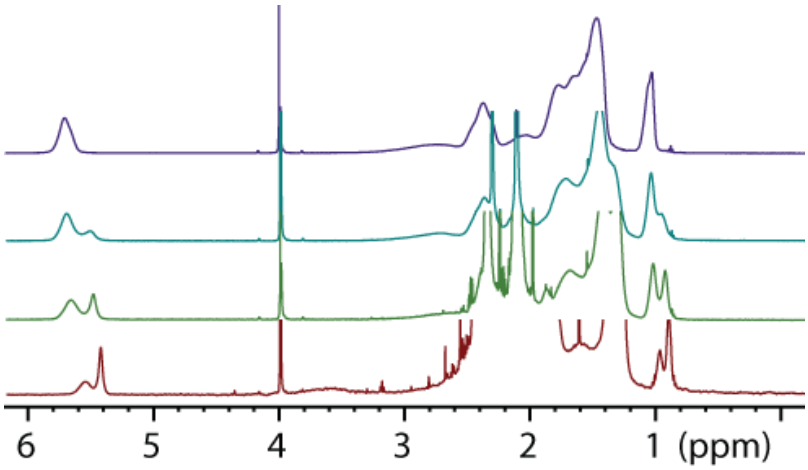

Figure S7. ^{1}H NMR spectra of PbSe nanocrystals (0.02 M in Carboxylate) dissolved in d_6-benzene in the presence of four concentrations of TMEDA (0.00 M (purple, top), 0.02 M (blue), 0.2 M (green), and 2.0 M (red, bottom)). Appearance of sharp vinyl peak corresponds to displacement of (κ^2-TMEDA)Pb(O_2CR)$_2$. Sharp resonance at δ = 4 ppm is from the ferrocene internal standard. Changes to the chemical shifts of both free and bound signals at high concentration of TMEDA added may be due to a change in the dielectric of the solvent medium. The final 2M concentration is ~20% /volume TMEDA. Similarly, as an increasing amount of Pb(O_2CR)$_2$ is removed from the nanocrystal the density of aliphatic ligands changes as does their local dielectric medium.

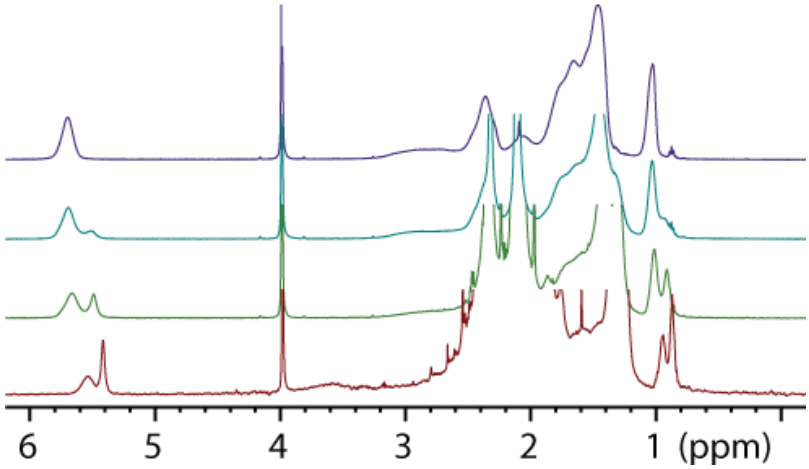

Figure S8 ^{1}H NMR spectra of PbS nanocrystals (0.02 M in Carboxylate) dissolved in d_6-benzene in the presence of four concentrations of TMEDA (0.00 M (purple, top), 0.02 M (blue), 0.2 M (green), and 2.0 M (red, bottom)). Appearance of sharp vinyl peak corresponds to displacement of (κ^2-TMEDA)Pb(O_2CR)$_2$. Sharp resonance at δ = 4 ppm is from the ferrocene internal standard. Changes to the chemical shifts of both free and bound signals at high concentration of TMEDA added may be due to a change in the dielectric of the solvent medium. The final 2M concentration is ~20% /volume TMEDA. Similarly, as an increasing amount of Pb(O_2CR)$_2$ is removed from the nanocrystal the density of aliphatic ligands changes as does their local dielectric medium.

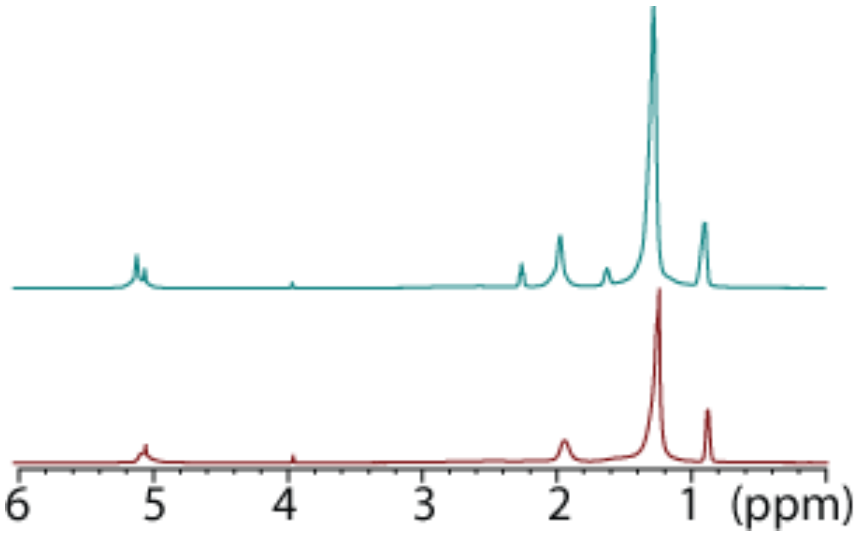

Figure S9. ^{1}H NMR spectra of CdSe nanocrystals dissolved in d_2-methylene chloride (red) and d_2-methylene chloride with 2.0 M pyridine added (blue). The chemical shifts of $Cd(O_2CR)_2$ bound to the nanocrystal and the pyridine-$Cd(O_2CR)_2$ complex have similar chemical shifts in d_2-methylene chloride, however sharp peaks for the methylene groups adjacent to the double bond of oleate are distinguishable enough to be integrated versus ferrocene. The percent of $Cd(O_2CR)_2$ removed by pyridine in methylene chloride (34%) is similar to the percent removed in benzene (40%). Z-type displacement does not depend heavily of the dielectric of the solvent.

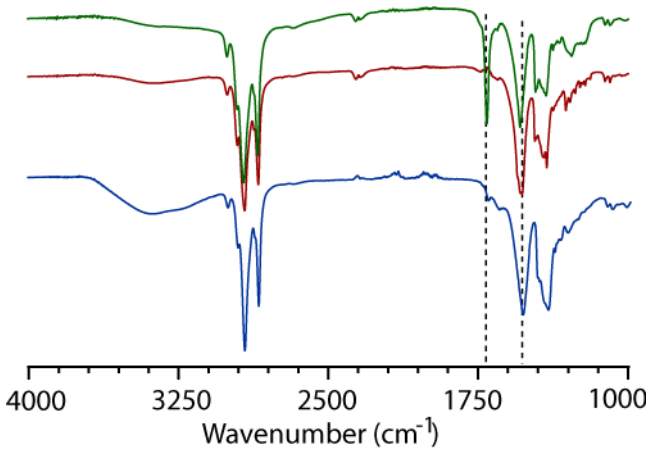

Figure S10: FT-IR spectra of $(CH_3OH)_n \bullet Cd(O_2CR)_2$ (R = oleyl, tetradecyl) isolated from CdSe nanocrystals after exposure to methanol (blue, bottom), oleic acid (green, top), and an independently prepared sample of cadmium tetradecanoate (red, middle). The broad band from 3000 - 3800 cm^{-1} in the isolated sample of $Cd(O_2CR)_2$ corresponds to the hydroxyl stretch of residual methanol.

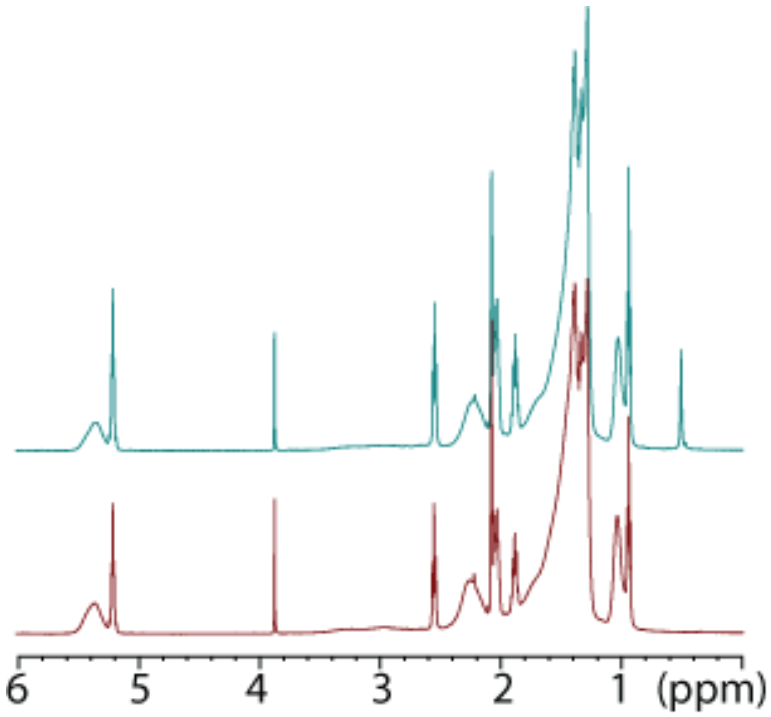

Figure S11. Temperature dependence of Z-type displacement with pyridine. ^{1}H NMR shows no decrease in the coverage of $Cd(O_2CR)_2$ after heating CdSe nanocrystals in a 2.0 M solution of pyridine and d_8-toluene to 100° C for 1 (red) to 5 hours (blue). Increasing the length of heating time does not influence the coverage of $Cd(O_2CR)_2$ showing that 40% coverage in 2.0 M pyridine is the equalibrium coverage.

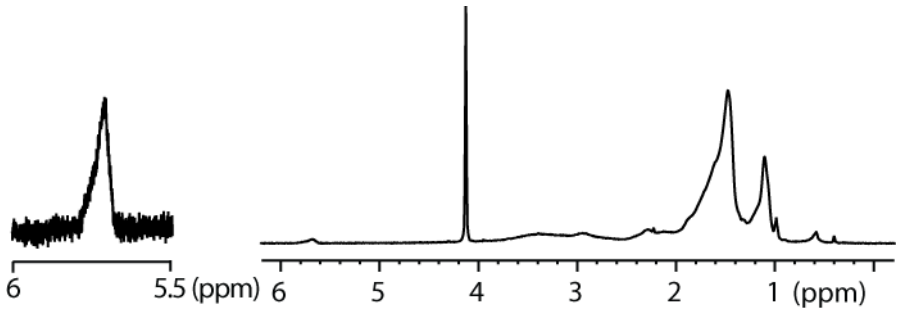

Figure S12. ^{1}H NMR spectrum of CdSe nanocrystals isolated after treatment with 1:1 mixture of TMEDA and *n*-octylamine showing signals from bound *n*-octylamine (180/nanocrystal, 5 nm^{-2}) as well as the vinyl resonance at δ = 5.7 ppm corresponding to 15 carboxyates/nanocrystal, 0.3 nm^{-2} (starting nanocrystals had a 2:1 ratio of oelyl tetradecyl). Signals from bound TMEDA are not apparent (for reference: δ = 2.2 - 2.6 ppm in (κ^2-TMEDA)Cd($O_2CR)_2$). Sharp resonance at δ = 4 ppm is from the ferrocene internal standard.

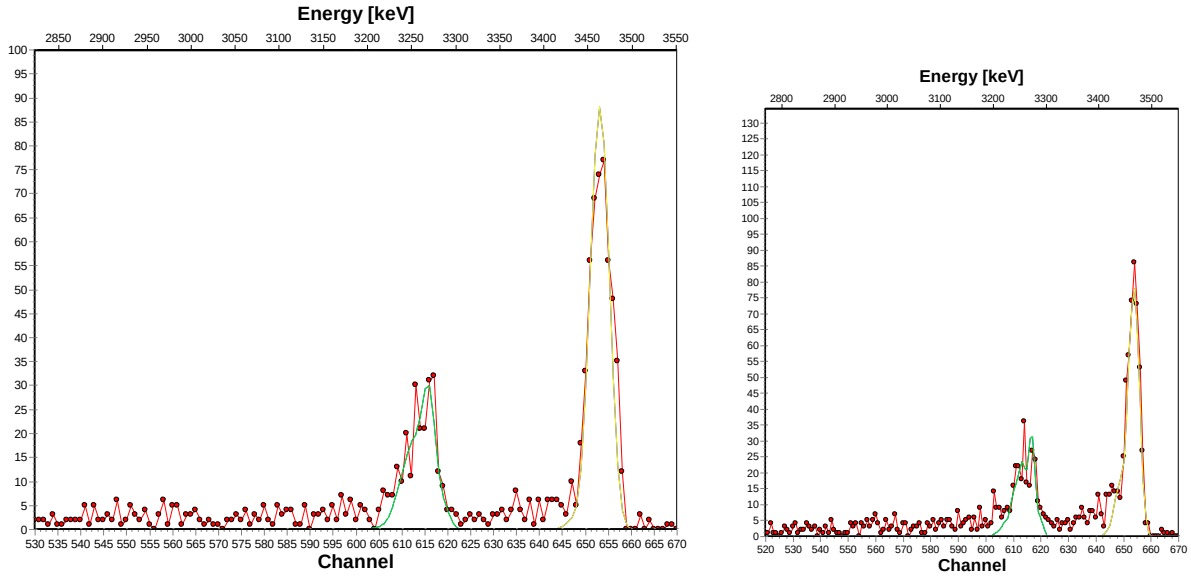

Figure S13. Rutherford backscattering spectra of isolated CdSe nanocrystals (left) and TMEDA-treated CdSe nanocrystals (right). The green line is a fit to the Se and the yellow line fits the Cd signal. Isolated CdSe nanocrystals have a Cd:Se ratio of 1.1, which decreases to 1.0 on treatment with TMEDA.

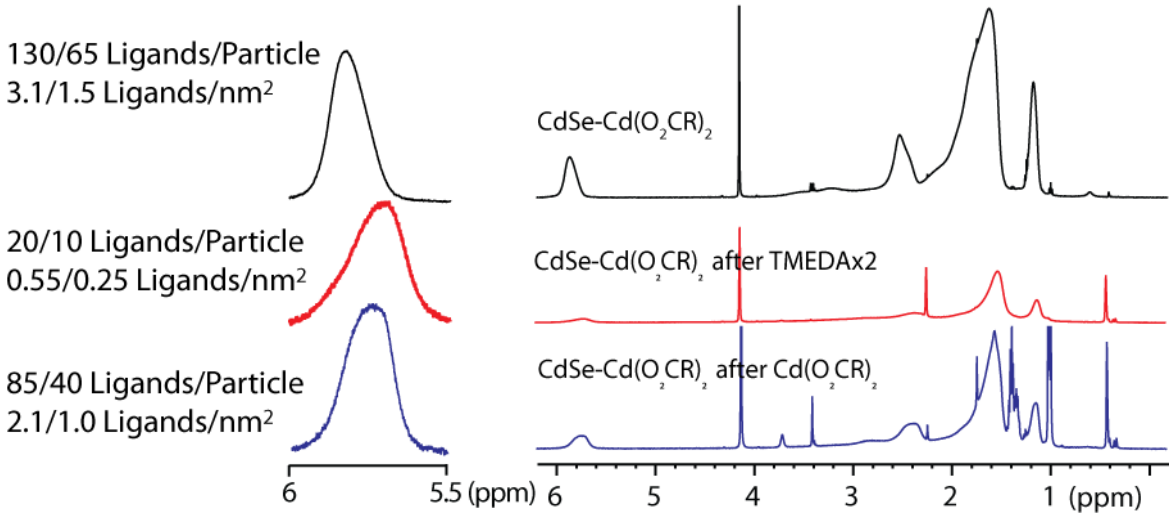

Figure S14 ^{1}H NMR spectra of CdSe nanocrystals after isolation (top, black), after partial displacement of the ligand shell by TMEDA and isolation (middle, red), and after $Cd(O_2CR)_2$ rebinding and isolation (bottom, blue). The left side shows an inset of the vinyl region normalized to the same intensity, and right side shows full ^{1}H NMR spectra normalized to the ferrocene standard. Ligand coverages are 3.1 nm^{-2} for the isolated CdSe nanocrystals (black), 0.6 nm^{-2} for the TMEDA-treated nanocrystals (red), and 2.1 nm^{-2} for the $Cd(O_2CR)_2$-treated nanocrystals (blue). Sharp resonance at δ = 4 ppm is from the ferrocene internal standard.

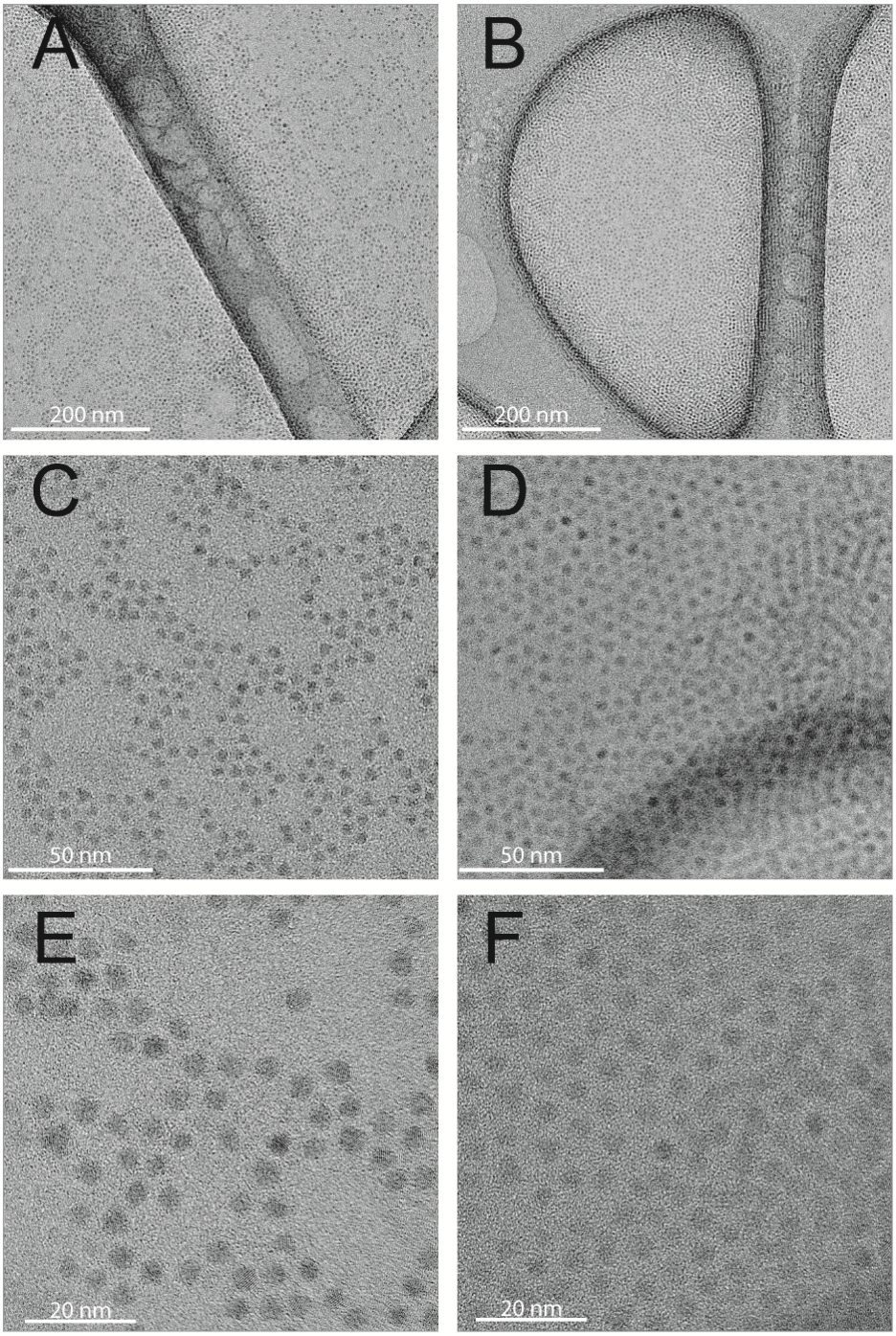

Figure S15. Transmission Electron Micrographs of CdSe nanocrystals with 3.3 carboxylates nm^{-2} (left column, A,C,E) and 0.6 carboxylates nm^{-2} (right column, B,D,F) at increasing magnification from top to bottom. Nanocrystal size and distance between nanocrystals does not change significantly as the ligand coverage is decreased, however the images do not have the resolution to determine small changes to the nanocrystal diameter.

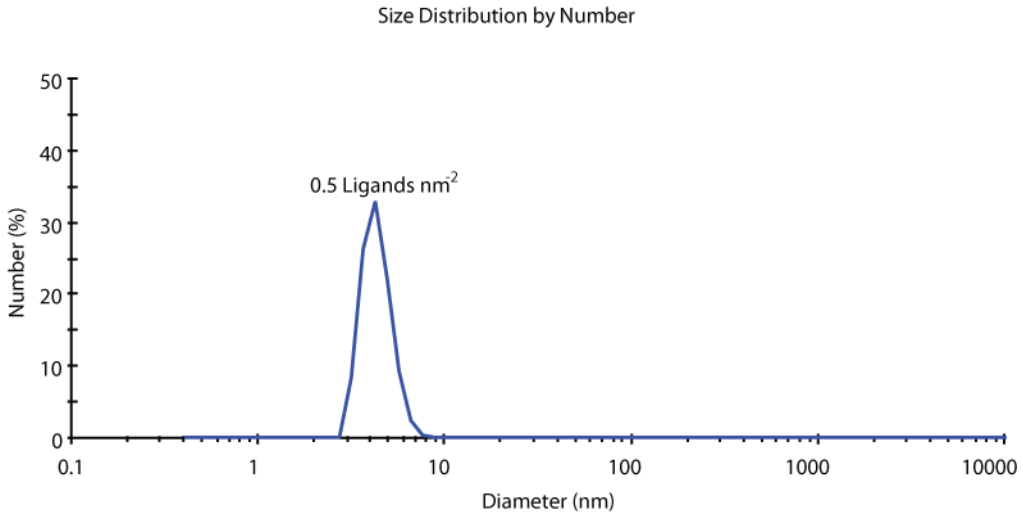

Figure S16 Dynamic light scattering histogram for CdSe nanocrystals with 0.6 carboxylates nm^{-2} showing no aggregation at this ligand coverage.

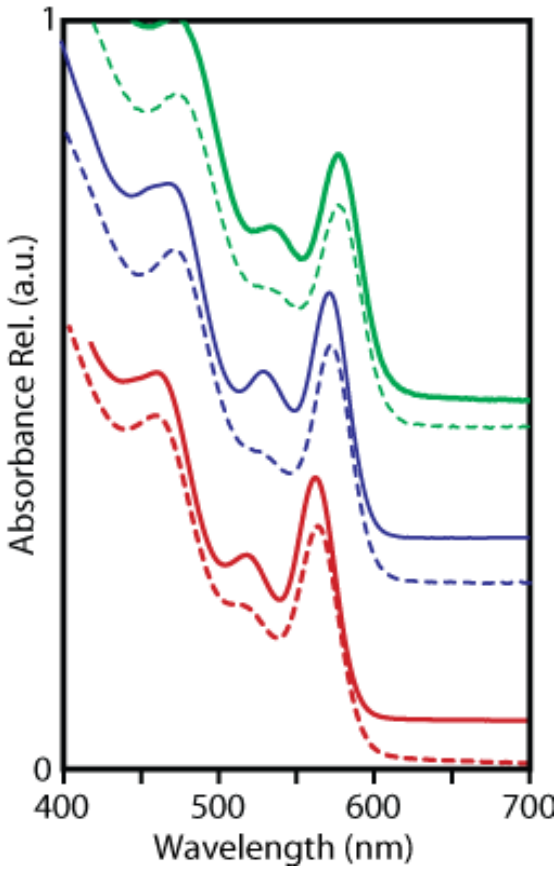

Figure S17. Changes to the absorbance spectrum of CdSe nanocrystals as a function of nanocrystal size. Nanocrystals of diameter d = 3.3 (red), 3.5 (blue), and 3.7 (green) with high (solid) and low (dotted) coverages of $Cd(O_2CR)_2$. No significant changes as a function of nanocrystal size are notable, i.e. the changes to the optical properties on removal of $Cd(O_2CR)_2$ do not depend on the size of the nanocrystal.

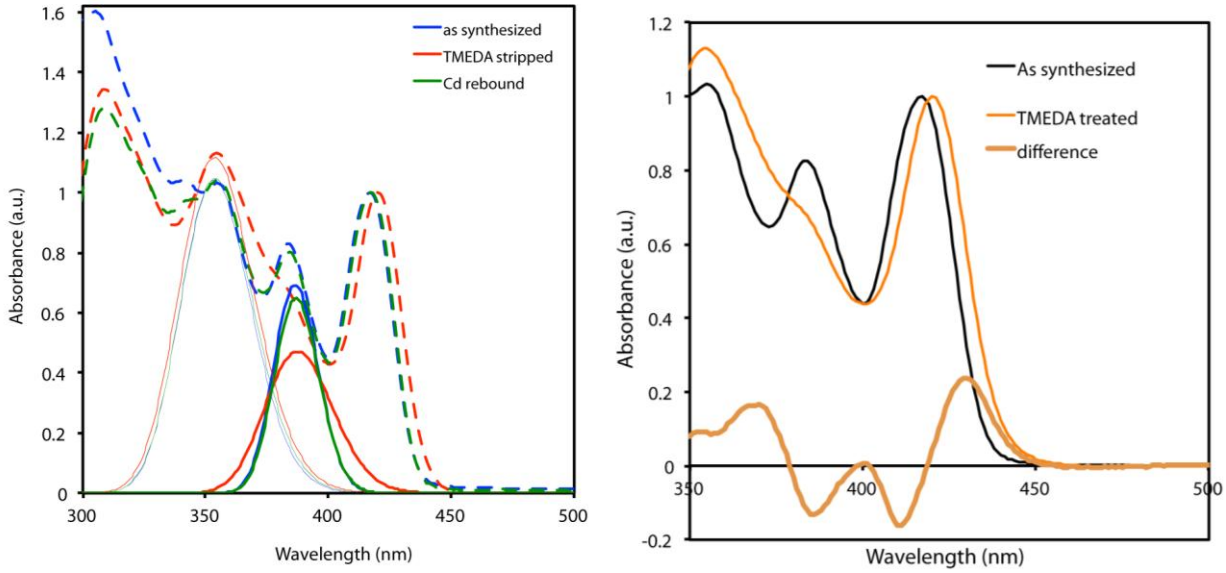

Figure S18: Left**:** Absorption spectra (dotted lines) for CdS nanocrystal normalized at the first transition and fit between 348 nm and 396 nm with two Gaussians (solid lines). As synthesized nanocrystals (blue) have a full-width half-maximum (FWHM) of 0.18 eV for the $1S_e$-$2S_{3/2}$ transition. Upon addition of TMEDA and removal of $Cd(O_2CR)_2$, the FWHM of the $1S_e$-$2S_{3/2}$ transition increases to 0.27 eV. Rebinding of cadmium oleate causes the $1S_e$-$2S_{3/2}$ transition to narrow to the original FWHM of 0.18 eV. Right: Difference between the absorption spectra for as-synthesized CdS nanocrystals (black) and isolated with TMEDA (orange). Curve is characteristic of a broadening $1S_e$-$2S_{3/2}$ transition. Integration of the normalized spectra in Figure 5 of the main text also indicates that the $1S_e$-$2S_{3/2}$ transition is broadening, as the total integral does not change with surface coverage.

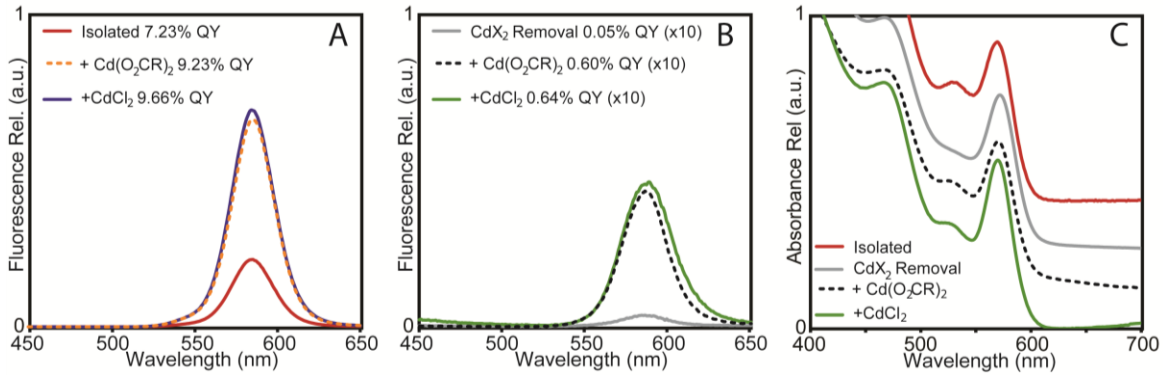

Figure S19: A. Changes to the photoluminescence spectrum of CdSe nanocrystals isolated by precipitation from pentane with methyl acetate (red, solid, PLQY = 7.2%, 3 $^{-}O_2CR$ nm^{-2}) on adding cadmium complexes $Cd(O_2CR)_2$ (orange, dashed, PLQY = 9.2%) and $CdCl_2$ (blue, solid, PLQY = 9.7%). Photoluminescence is normalized by quantum yield. Addition of CdX_2 to isolated CdSe nanocrystal samples increases PLQY by ~25%. **B.** Changes to the photoluminescence spectrum of CdSe nanocrystals isolated by precipitation from a 0.5 M solution of Bu_3P in pentane using methyl acetate (grey, solid, PLQY = 0.1%, 1 $^{-}O_2CR$ nm^{-2}) on addition of $Cd(O_2CR)_2$ (black, dashed, PLQY = 1%) and $CdCl_2$ (green, solid, PLQY = 1%). PLQY increase an order of magnitude on addition of CdX_2. All spectra are normalized by PLQY and multiplied 10x compared with panel A. **C.** UV-visible spectroscopy for CdSe nanocrystals isolated by precipitation from pentane with methyl acetate (red, solid, top, 3 $^{-}O_2CR$ nm^{-2}) and CdSe nanocrystals isolated by precipitation from a 0.5 M solution of Bu_3P in pentane using methyl acetate (grey, solid, top-middle, 1 $^{-}O_2CR$ nm^{-2}) with added $Cd(O_2CR)_2$ (black, dashed, bottom-middle) and $CdCl_2$ (green, solid, bottom). Removal of $Cd(O_2CR)_2$ using Bu_3P causes the apparent intensity of the $1S_e$-$2S_{3/2}$ transition to decrease, but it is partially recovered on saturation with CdX_2. Some scattering is visible at longer wavelengths due to poor solubility of these CdX_2 salts in toluene.

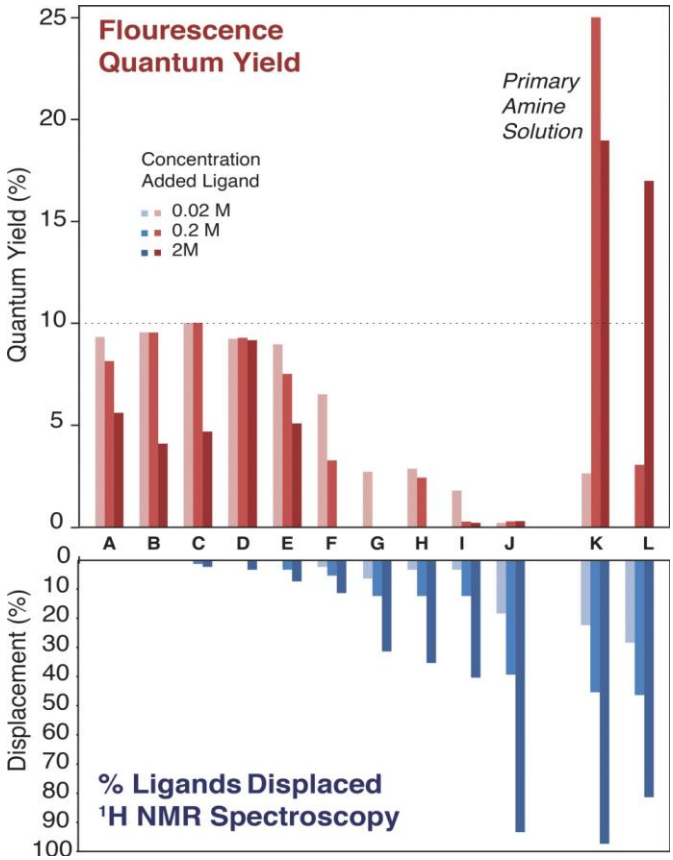

Figure S20: Graph depicting PLQY (top, red) and $Cd(O_2CR)_2$ displacement (bottom, blue) as a function of ligand concentration for methyl acetate (A), nonanyl nitrile (B), Bu_3N (C), tetrahydrofuran (D), tetradecanol (E), N,N-dimethyl-*n*-butylamine (F), Bu_3P (G), N,N,N',N'-tetramethylbutylene-1,4-diamine (H), pyridine (I), TMEDA (J), *n*-octylamine (K), and a 50:50 (mol) mixture of TMEDA and *n*-octylamine (L). Loss of $Cd(O_2CR)_2$ decreases PLQY, except in the case of primary amines, which tightly bind the nanocrystal surface.

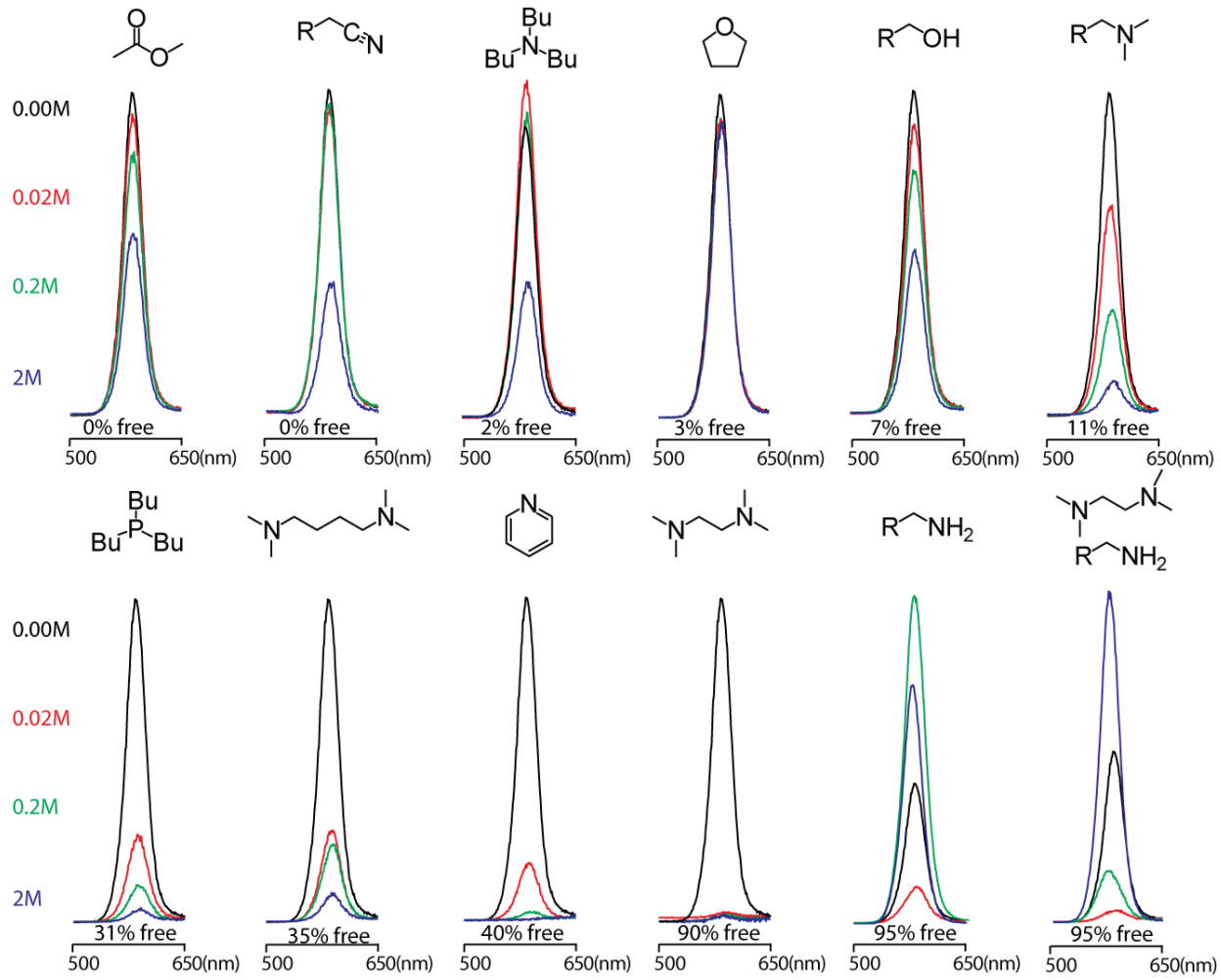

Figure S21. Normalized photoluminescence spectra for CdSe nanocrystals treated with various Lewis bases used to compile Figure 4 of the main text. Changes to the photoluminescence were monitored at 0.00 M (black), 0.02 M (red), 0.20 M (green), and 2.0 M (blue). In general, increasing the concentration of Lewis bases quenches photoluminescence depending on the ability of the base to remove $Cd(O_2CR)_2$, with the exception of the primary amine solutions, where photoluminescence is initially quenched but then increases as amines bind the nanocrystal surface.

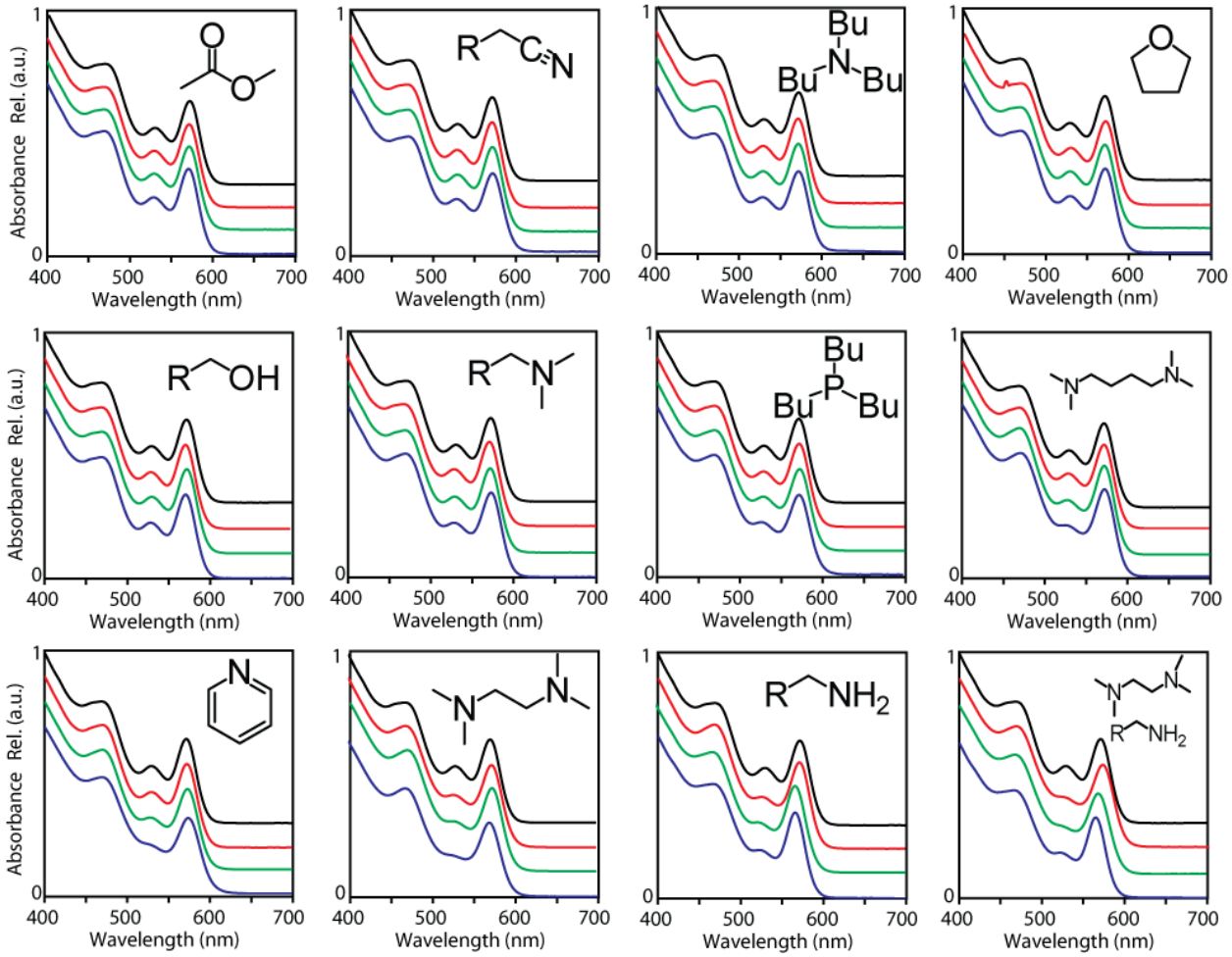

Figure S22. UV-visible absorption spectra for CdSe nanocrystals treated with various Lewis bases. Changes to the UV-visible spectra were monitored at 0.00 M (black), 0.02 M (red), 0.20 M (green), and 2.0 M (blue). In general, increasing the concentration of Lewis bases broadens the $1S_{e}$-$2S_{3/2h}$ depending on the ability of the base to remove $Cd(O_2CR)_2$, with the exception of the primary amine solutions, where $1S_{e}$-$2S_{3/2h}$ is initially broadened but then narrows as amines bind the nanocrystal surface. All spectra are normalized to 350 nm and offset.

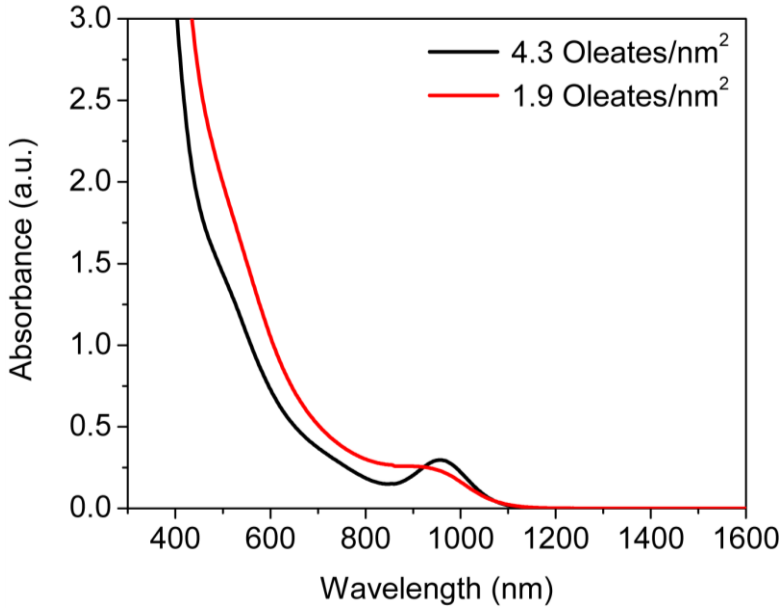

Figure S23. UV-visible absorption spectra for PbS nanocrystals (d = 3.1 nm) before (black) and after (red) treatment with excess TMEDA. The absorption blue-shifts and broadens as the coverage of lead oleate decreases.

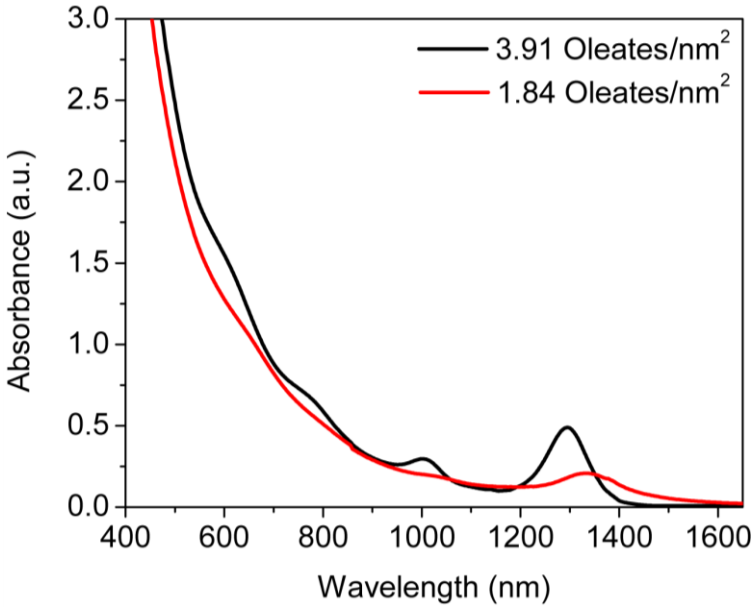

Figure S24. UV-visible absorption spectra for PbSe nanocrystals (d = 3.8 nm) before (black) and after (red) treatment with excess TMEDA. The absorption red-shifts and broadens as the coverage of lead oleate decreases.